



THE UNIVERSITY *of* EDINBURGH

Edinburgh Research Explorer

Power capacity profile estimation for building heating and cooling in demand-side management

Citation for published version:

Gomez, JA & Anjos, MF 2017, 'Power capacity profile estimation for building heating and cooling in demand-side management', *Applied Energy*, vol. 191, pp. 492-501.
<https://doi.org/10.1016/j.apenergy.2017.01.064>

Digital Object Identifier (DOI):

[10.1016/j.apenergy.2017.01.064](https://doi.org/10.1016/j.apenergy.2017.01.064)

Link:

[Link to publication record in Edinburgh Research Explorer](#)

Document Version:

Peer reviewed version

Published In:

Applied Energy

General rights

Copyright for the publications made accessible via the Edinburgh Research Explorer is retained by the author(s) and / or other copyright owners and it is a condition of accessing these publications that users recognise and abide by the legal requirements associated with these rights.

Take down policy

The University of Edinburgh has made every reasonable effort to ensure that Edinburgh Research Explorer content complies with UK legislation. If you believe that the public display of this file breaches copyright please contact openaccess@ed.ac.uk providing details, and we will remove access to the work immediately and investigate your claim.



Power Capacity Profile Estimation for Building Heating and Cooling in Demand-Side Management

Juan A. Gomez^{a,*}, Miguel F. Anjos^a

^aGERAD and Department of Mathematics and Industrial Engineering, Polytechnique Montreal, C.P. 6079, Succ. Centre-Ville, Montreal, QC, Canada H3C 3A7

Abstract

This paper presents a new methodology for the estimation of power capacity profiles for smart buildings. The capacity profile can be used within a demand-side management system in order to guide the building temperature operation. It provides a trade-off between the quality of service perceived by the end user and the requirements from the grid in a demand-response context. We use a data-fitting approach and a multiclass classifier to compute the required profile to run a set of electric heating and cooling units via an admission control module. Simulation results validate the performance of the proposed methodology under various conditions, and we compare our approach with neural networks in a real-world-based scenario.

Keywords: Smart buildings, power demand, residential load sector, least squares, parameter estimation, classification.

1. Introduction

In the context of power systems, reducing peaks and the fluctuation of consumption brings stability to the system and benefits to the players in the power supply network. In this respect, demand-response (DR) programs and demand-side management (DSM) systems encourage and facilitate the participation of the end users in the grid decisions. This participation is increasing with the development and implementation of smart buildings. DR programs have mostly been oriented to large consumers, but smart buildings can exploit the DR potential in residential and commercial buildings as well. These represent around 70% of the total energy demand in the United States [1]. In Canada, space heating is responsible for more than 60% of the total residential energy consumption, due to the cold climate [2]. Across the country, electric baseboards account for 27% of heating equipment, reaching 66% in the province of Quebec. On the other hand, the province of Ontario is typically a summer-peaking region due to the high temperatures during that season and the high penetration of air-conditioning systems [3, 4].

Several authors have published DSM-related results. Normally their research motivation is oriented to load management, user behavior, cost performance, and curve shaping. Imposing a capacity constraint is a common idea among these approaches. Costanzo et al. [5] propose a multilayer architecture that provides a scheme for online operation and load control given a maximum consumption level. In the stochastic DSM program in [6], a DR

aggregator imposes a capacity constraint. Bidding curves and price analyses are reported in order to guide end-users about increasing capacity. Rahim et al. [7] evaluate the performance of several heuristic-based controllers. They define the load management as a knapsack problem with preset power capacities for each time slot. In a similar way, [8] assumes a consumption limit that allows the activation of only one load at a time. Li et al. [9] look for an optimal allocation of capacities based on a queueing strategy. The service provider determines the capacity to assign to each user from a set of renewable resources.

The idea of capacity subscription is explored in [10], where the individual consumer's demand is limited in a competitive market. On the other hand, the heuristic algorithm proposed in [11] aims to minimize the error between the actual power curve and the objective load curve by moving the shiftable loads. In this case the objective load curve can be seen as a soft constraint capacity profile.

A variation of the capacity limit is presented in [12], where each individual user has a predefined budget to maximize his/her satisfaction.

All the approaches mentioned represent the capacity as a given parameter, and some of them recognize the importance of using a forecasting tool to determine its value. Estimating the user consumption is a key step in the decision-making process for users and for higher levels in the power system. Relevant publications can be found in the load-forecasting literature. Suganthi and Samuel [13] give a comprehensive review of forecasting methods from classical time series to more sophisticated machine learning tools.

Load estimation methods are classified depending on the level of aggregation of the input data: they can be

*Corresponding author

Email address: juan.gomez@polymtl.ca (Juan A. Gomez)

bottom-up or top-down [14]. Bottom-up models extrapolate the behavior of a larger system based on its inner elements. Top-down models make decisions from a global perspective and share them among all the subsystems.

Notation

$h \in \{1, 2, \dots, H\}$	Set of time frames in horizon.
$t \in \{1, 2, \dots, S\}$	Set of time steps in time frame h (same for every h).
$i \in \{1, 2, \dots, I\}$	Set of loads.
N_h	Number of requests received in time frame h .
P_i	Power level of load i (kW).
C_h	Power capacity in time frame h (kW).
$r_{i,t}$	$\begin{cases} 1 & \text{if a request is created by load } i \text{ in time step } t \\ 0 & \text{otherwise} \end{cases}$
$x_{i,t}$	$\begin{cases} 1 & \text{if request from } i \text{ is accepted in time step } t \\ 0 & \text{otherwise} \end{cases}$
QoS_h	Quality of service in time frame h .
\widehat{QoS}_h	Quality of service of the prediction model in time frame h .
T	Temperature ($^{\circ}\text{C}$).
T_h^e	External temperature in time frame h ($^{\circ}\text{C}$).
\mathcal{P}	Power levels of the loads in each scenario.
Ω	Discrete set of capacities.
$\omega \in \Omega$	Capacity class.

Within these two categories different approaches have been used to estimate the energy demand. Ahmed et al. [15] compare artificial neural networks and the autoregressive integrated moving average, showing the effect on the scheduling of storage devices. Jain et al. [16] use support vector regression to evaluate the impact of the time and space granularity inside a multi-family unit. Al-Wakeel et al. [17] use a k -means-based load estimation method to compute future load profiles using complete and incomplete past information.

Logistic and Poisson regression are used in [18] to estimate energy demand in a large aggregated population. In a similar way, [19] presents a short-term forecasting method for aggregated loads, specifically in buildings with daily or seasonal patterns of consumption. Mohajeryami et al. [20] present an error analysis for different load estimation methods that are used in real-world operations. They highlight the importance of an accurate estimation for exploiting the DR potential.

On the other hand, when the prediction output belongs to a discrete set of categories the estimation can be defined

as a classification problem. Some related energy problems are treated in this way: price forecasting in [21] and wind power ramp events in [22].

This paper proposes an approach for the estimation of a power capacity profile that works in combination with the admission controller (AC) module presented in [5]. This profile is used to ensure enough power to meet the demand for the next planning horizon (e.g., the next day in a day-ahead DR market). This novel approach takes advantage of the structure derived from the estimation problem to compute capacity profiles efficiently and reliably. Estimating the capacity that will be necessary allows us to define a relationship between the total expected demand and the level of service the user desires while providing DR. In this scenario the user will book a variable maximum power capacity per time frame over the planning horizon, ensuring a pre-established level of service. This approach could also include external factors such as peak control and pricing policies. The motivation is that a defined power *budget* limits the consumption and encourages load shifting. It also facilitates the integration of differential pricing for both energy and power.

This paper is structured as follows. We describe the proposed methodology in Section 2. We give simulation results for the real-world-based scenario in Section 3, and Section 4 presents our conclusions.

2. Power Capacity Profile

Figure 1 shows the application of the AC module presented in [5]. The online algorithm in the AC has four stages. First, the space heaters and the air conditioners create requests $r_{i,t}$ when the room temperature is out (or going out) of the thermal comfort zone. Second, the algorithm sorts all the requests from the highest to the lowest priority value; the priority value is the normalized difference between the temperature in the room and the external temperature. Third, the AC accepts the highest priority requests until the given capacity C_h is consumed; the other requests are rejected. Finally, it sends the signal $x_{i,t}$ back to each smart load i either to run (if accepted) or to stand by for the next time step (if rejected).

Figure 2 presents a basic example of the AC operation. A smart house with two rooms, R1 and R2, is simulated over a horizon of 5 time frames. Each time frame has 10 time steps where the smart loads can send requests. Typically, a time frame would be equivalent to an hour in a realistic scenario. There is a 1.5 kW space heater in each room, and the external temperature is 5°C (Figure 2(a)).

We can see the peak reduction obtained by the AC in Figure 2(b); the end-user agrees to have a preset power capacity (dashed red line), which constrains the consumption to at most 1.5 kW. The peak of consumption, for this example 3 kW, would be attained when the two space heaters are being used at the same time step. Figures 2(c) and 2(d) show the internal temperature in each room within a certain comfort zone. In a similar way, we can see the

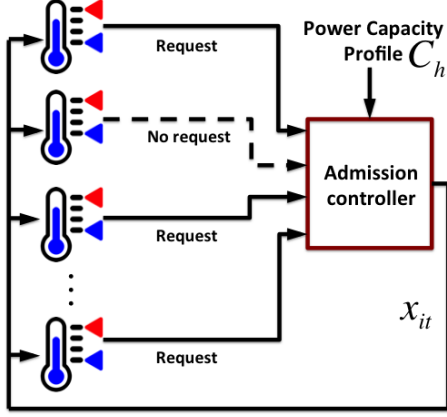


Figure 1: Admission controller.

time steps where the heaters are working in Figures 2(e) and 2(f). For more details about the AC algorithm and the heat transfer equations we refer the reader to [5].

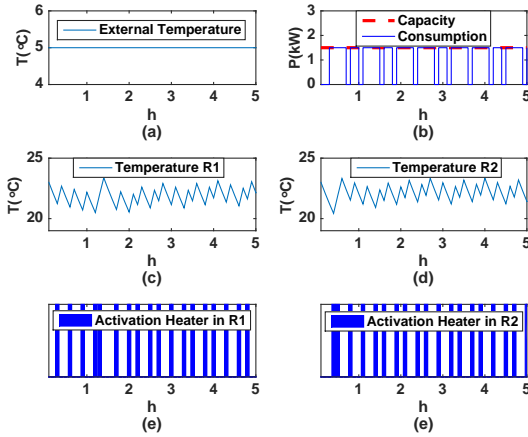


Figure 2: Example of results from admission controller.

In the previous example the capacity profile suffices to keep the average internal temperatures $(21.8, 22.2)^\circ\text{C}$ in the comfort zone $[20 - 24]^\circ\text{C}$. In the event that the temperature in a room goes out of the comfort zone during a time step, the space heater will increase its priority value, and the AC will accept the request in the next time step. The capacity profile also achieves a peak shaving effect. However, alternating the use of the heaters might not be enough to ensure a comfortable internal temperature if the external temperature is extremely low; a higher capacity profile might be required. This decision becomes more complex if we increase the number of space heaters and if they have different power requirements.

We introduce the quality of service (QoS) index to quantify the impact of a given capacity on the whole system. The general idea of QoS is that the user should be willing to pay more if a higher level of service is desired. This decision-making by the user is especially important

under time-of-use pricing conditions because the customer can profit from the cheaper time frames by reshaping the load curve while ensuring the desired QoS .

In a smart building it is possible to compute the QoS from the information provided by thermostats and smart loads connected to the AC. In the spirit of [23], we define the QoS for each time frame h as follows:

$$QoS_h = \begin{cases} \frac{\sum_{i=1}^I \sum_{t=1}^S x_{i,t}}{N_h} \times 100\% & N_h > 0 \\ 100\% & N_h = 0, \end{cases} \quad (1)$$

where $N_h = \sum_{i=1}^I \sum_{t=1}^S r_{i,t}$.

The accepted requests have to satisfy

$$\sum_{i=1}^I x_{i,t} P_i \leq C_h \quad \forall t \in \{1, 2, \dots, S\}. \quad (2)$$

Equation (2) indicates that the AC accepts requests until the capacity limit is reached. In the framework of this article we assume that both air-conditioning units and electric baseboard heaters have a constant level of consumption [24]. Let $C_h \in \Omega$, where Ω is a set of capacities that can work in combination with the AC and the set of loads. In other words, we do not want a capacity to operate a fractional number of loads in the time step t . Given that Ω is a discrete set we can define the classification problem

$$\Phi(T_h^e, QoS_h) = C_h \quad (3)$$

that determines $C_h \in \Omega$ for a given external temperature T_h^e and the QoS_h defined by the user. We solve this classification problem using a three-step approach: selection of the training set from historical data, function fitting, and final classification. We illustrate the steps in this section with a group of space heaters; Section 3 includes experimental results for both types of loads.

2.1. Sampling From Historical Data

The real data is obtained from the smart energy management system, which records the accepted requests, the rejections, and the evolution of the QoS over time. We simulate this historical data to understand the system dynamics and to implement a prediction model. The simulation conditions are:

- The set of heaters is composed of four identical units of 1.5 kW of consumption.
- The heat transfer is computed using the specific heat and Fourier's law formulations implemented in [5] (see Section 3 for more details).
- The external temperature corresponds to the complete year 2013 (8760 hours) in the Montreal area [25].

- The comfort intervals for the internal temperatures are taken from the ISO 7730 standard analyzed in [26]. For an *office category B* the intervals are $[20 - 24]^{\circ}\text{C}$ and $[23 - 26]^{\circ}\text{C}$ for heating and cooling respectively.
- C_h is randomly chosen from $\Omega = [1.5, 3.0, 4.5, 6.0]$ based on the interval of temperature; the highest capacities are not necessary during the warmer days (for example, with $T_h^e = 19^{\circ}\text{C}$ every value in Ω will return a QoS_h near 100%, affecting the quality of the data training set and the estimation).

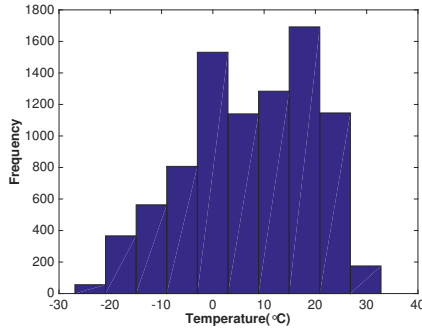


Figure 3: Histogram of hourly external temperatures in Montreal, Canada for 2013.

Figure 3 shows the frequency of the external temperature intervals in the historical data; this is clearly an imbalanced set. This imbalance is generated by the similar weather in Spring and Fall. The temperatures between 0 and 20°C would have a significantly higher weight in a fitting process. We use random under-sampling [27] in order to match the number of points in the minority group from the temperatures below the comfort interval.

Figure 4 shows the hourly QoS results for the balanced set. We can identify several characteristics of the system behavior:

- As the temperature increases the QoS converges to higher values; with fewer requests the selection of a capacity level is a less sensitive issue.
- The selection of the capacity level has a big impact on the QoS in lower temperature conditions.
- The QoS seems to behave asymptotically for higher and lower temperatures.

2.2. Data Fitting

Once we have identified these features in the data set we can solve an optimization problem for the capacity estimation. We fit the sigmoid function

$$\widehat{QoS}_h = \frac{\beta_1}{1 + e^{\beta_2 T_h^e}} + \beta_3 C_h + \beta_4, \quad (4)$$

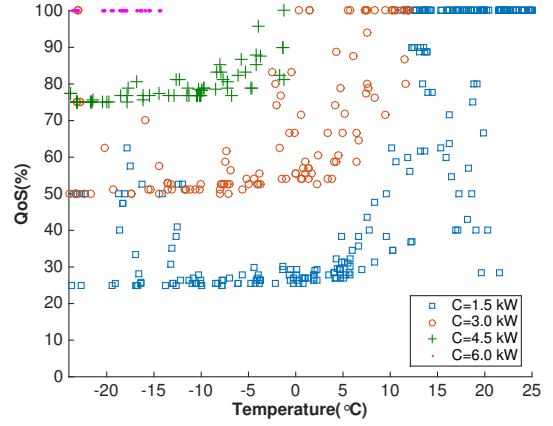


Figure 4: Graph of QoS vs. temperature for the sampled historical data.

where \widehat{QoS}_h is the quality of service from the prediction model at time frame h .

Additionally, we will compare two different optimality criteria: the least squares value (LSV) and the least absolute value (LAV). Typically, the LSV gives more weight to distant points while the LAV is resistant to outliers [28].

The optimization problems are:

$$\min_{\beta_1, \beta_2, \beta_3, \beta_4} \sum_{h=1}^H (QoS_h - \widehat{QoS}_h)^2 \quad (5)$$

$$\min_{\beta_1, \beta_2, \beta_3, \beta_4} \sum_{h=1}^H |QoS_h - \widehat{QoS}_h| \quad (6)$$

Figure 5 shows the results for a least-squares fitting of a sigmoid function.

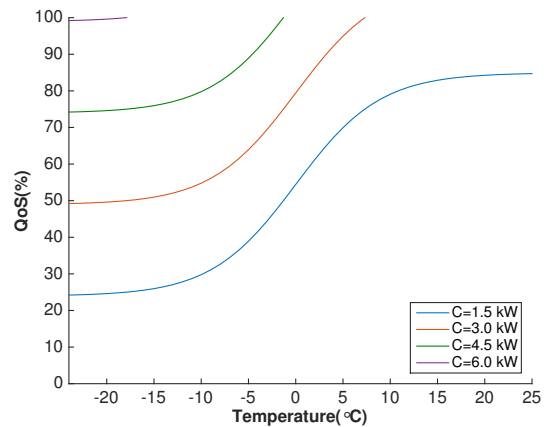


Figure 5: Fitted sigmoid function.

Once we have solved the optimization problem (5) or (6) we can use (4) to compute the expected required capacity for the desired QoS .

2.3. Motivation for Using a Sigmoid Function

The selection of a sigmoid function has both a graphical justification and an interesting background. We provide intuition into why it works for the heating case; the cooling case is similar. This analysis applies to any external temperature regardless of the time frame where it occurs; therefore we omit the subscript h and use N in the place of N_h to increase readability.

We make the following assumptions:

- If $T^{e'} < \hat{T}^e$ then $N(T^{e'}) > N(\hat{T}^e)$ for any temperatures $T^{e'}$ and \hat{T}^e .
- $C \in [C_{\min}, \infty)$ where $C_{\min} = \max(P_i)$.
- Each load generates at most one request per time step, and therefore the maximum number of requests per step equals I .
- There exists a temperature \tilde{T}^e at which all the heaters generate requests at every time step, and therefore $N(\tilde{T}^e) = I \times S$.

Considering the worst-case scenario for any time frame in Equations (1) and (2), we have:

$$QoS(\tilde{T}^e, C_{\min}) = \frac{\sum_{i=1}^I \sum_{t=1}^S x_{i,t}}{I \times S} \quad (7)$$

$$\sum_{i=1}^I x_{i,t} P_i \leq C_{\min} \quad \forall t \in \{1, 2, \dots, S\} \quad (8)$$

Equation (8) allows us to accept at least one request at every time step. Therefore, the total number of accepted requests satisfies:

$$\sum_{t=1}^S \sum_{i=1}^I x_{i,t} \geq S. \quad (9)$$

After substituting (9) into (7) we can obtain a minimum QoS :

$$QoS(\tilde{T}^e, C_{\min}) \geq \frac{1}{I} \quad (10)$$

We can see similar behavior for scenarios with temperature $\tilde{T}^e > \hat{T}^e$ and $N(\tilde{T}^e) < N(\hat{T}^e)$. Let F be the minimum number of time steps where requests are received. Since each load i will request at most once per time step, we have:

$$F = \left\lceil \frac{N(\tilde{T}^e)}{I} \right\rceil = \frac{N(\tilde{T}^e)}{I} + \alpha, \quad 1 > \alpha \geq 0. \quad (11)$$

The variable F also becomes the minimum number of accepted requests due to the C_{\min} in Equation (8). By substituting (11) into (1) we obtain:

$$QoS(\tilde{T}^e, C_{\min}) = \frac{\sum_{i=1}^I \sum_{t=1}^S x_{i,t}}{N(\tilde{T}^e)} \geq \frac{F}{(F - \alpha)I}. \quad (12)$$

When $\alpha = 0$ we get the same condition as in Equation (10).

A sigmoid function helps to represent the asymptotic extremes and monotonic behavior of the QoS . In the first case, we see how the QoS is bounded below in Equations (10) and (12), and it is bounded above by definition ($QoS \leq 100$). In the second case, the temperature and requests are inversely proportional (if $T^{e'} < \hat{T}^e$ then $N(T^{e'}) > N(\hat{T}^e)$), so $QoS(T^e)$ is monotonically increasing. Using a linear function would capture the monotonic condition but not the asymptotic extremes.

For cooling systems we would change the first assumption to $T^{e'} > \hat{T}^e$, giving $N(T^{e'}) > N(\hat{T}^e)$. This leads to a similar monotonically decreasing sigmoid function over the interval of external temperature where cooling is required.

2.4. Classification

As stated previously, we have a discrete set of capacities that are suitable for the performance of the system. We solve for C_h in (4) in order to compute the continuous signal \hat{C}_h . Finally, we use the multiclass classifier

$$C_h = \arg \min_{\omega \in \Omega} |\hat{C}_h - \omega| \quad (13)$$

to find the required capacity.

Figure 6 shows the effect of the classifier; it assigns areas to each of the capacities based on the midpoints for each pair of sigmoid curves from Figure 5.

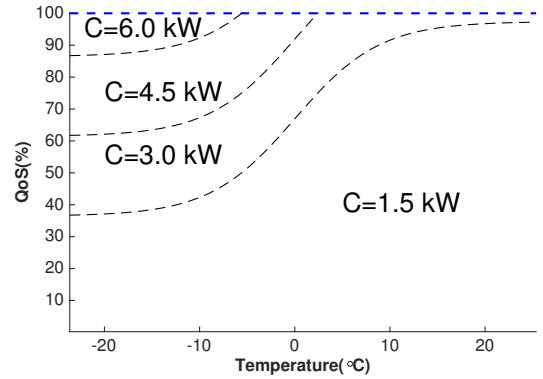


Figure 6: Classification areas.

3. Experimental Results

In the previous section we introduced the methodology with an example for a given set of homogeneous space heaters. In this section we carry out several experiments to assess and validate the performance of the proposed methodology under different conditions.

It is important to ensure **coherence in the thermal system when defining the set of loads**. The loads must keep the temperature in the comfort range during the warmest and coldest time frames in the data sets. This design step must include the specific features of the building such as

size, surfaces in contact with external temperatures, wall insulation materials, and thermal load inside the room. A poorly balanced thermal system could lead to a QoS of 100% with temperatures far from the comfort zone.

At the end of each time step, we compute the temperature in the rooms using the same thermal equations as in [5]:

$$\frac{dQ^{tot}}{dT^{room}} = m_{room}C_{room}, \quad (14)$$

$$\frac{dQ^{exch}}{dt} = -K_{wall} \frac{A}{\chi} (T^e - T^{room}), \quad (15)$$

$$Q^{tot} = Q^{exch} + \eta P_i, \quad (16)$$

where $K_{wall} = 4.8 \times 10^{-4}$ kW/m · °C is the average thermal conductivity of the wall, and $\eta = 100\%$ is the efficiency of the loads. We choose a room size of 60 m³, which corresponds to an air mass of $m_{room} = 72$ kg with a specific heat capacity $C_{room} = 1.0$ kJ/Kg · °C. The surface area in contact with the external temperature is $A = 12$ m² with a thickness of $\chi = 0.2$ m. This remains constant for all the experiments.

For a more realistic scenario both types of loads are managed by the AC; the space heaters and the air conditioners will create requests when the temperature in each room is moving out of the comfort zone.

The experiments include:

- Sets \mathcal{P} with homogeneous and heterogeneous power P_i values.
- Three different types of Ω sets: computed from all possible combinations of values in \mathcal{P} ; computed from some of the combinations in \mathcal{P} ; and given by an external entity.
- Two fitted functions.
- Two optimality criteria: LAV and LSV.
- Comparison with two neural networks (NNs) with different topologies.

The experiments are carried out in two stages. In the training stage we reproduce the approach presented in Section 2 in order to determine the classification areas. Then in the test stage we use the classification areas to estimate the capacity profiles for given levels of the QoS . When the profiles have been computed, we run a simulation to verify the actual QoS performance.

In Sections 3.1 and 3.2 we illustrate the methodology on a three-load instance: an apartment with three rooms. In Section 3.3 we report results for an instance with 50 loads to demonstrate the scalability of our methodology.

3.1. Training for Three-Load Instance

We required two training sets: one for heaters and one for air conditioners. Each training set is defined over the corresponding interval of temperature ($T_h^e \leq 20^\circ\text{C}$ for heaters and $T_h^e \geq 26^\circ\text{C}$ for air conditioners) and randomly chosen as in Subsection 2.1. The historical sets are simulated using the hourly temperature in Montreal for the year 2013 (8760 data points).

As mentioned before, we will compare this methodology with two other approaches. In the first case, we use the polynomial function

$$\widehat{QoS}_h = \beta_1 + \beta_2 C_h + \beta_3 T_h^e + \beta_4 T_h^e C_h \quad (17)$$

in the fitting step. A priori the sigmoid function gives a better representation of the historical set due to its monotonically increasing behavior and the asymptotic extremes. The function in Equation (17) captures only the monotonic condition. To fit each function we solve a nonlinear optimization problem using the BFGS method; it finds a solution in a few seconds.

We use NNs, which are widely used in many different types of problems, as a second benchmark. For classification problems the NN typically has the same number of neurons in the output layer as the number of classes. The NN computes the probability that each input belongs to each class, and it chooses the class with maximum probability. We implemented two NNs with $A = 1$ and $B = 2$ hidden layers (5 neurons each), cross entropy as a performance measure in the learning process, and a validation subset of 30% of the points. The training time of the NNs varies between 10 and 20 seconds using scaled conjugate gradient backpropagation.

Finally, the total confusion or missclassification index measures the performance of each approach. It indicates the percentage of the total set of data that was incorrectly classified.

Tables 1 and 2 show the training results for the different scenarios and approaches. Scenarios 1–7 and 8–14 correspond to heating and cooling respectively. In scenarios 1–3 and 8–10 the loads are homogeneous and the Ω set corresponds to all possible combinations of the loads. In scenarios 4–6 and 11–13, both homogeneous and heterogeneous loads are tested with a Ω set that was defined separately from the loads. Finally, scenarios 7 and 14 contain a heterogeneous set of loads and all possible combinations in Ω .

In general, we observe a better performance in the sigmoid fitting (SLAV and SLSV) than in the polynomial cases (PLAV and PLSV). There is no clear difference in terms of the fitting criterion. The sigmoid function seems to be competitive with both NNs in the first six scenarios of each table.

As stated before, the sigmoid function provides a better representation of the structure of the problem. Figure 7 shows the classification areas obtained by fitting the sigmoid and polynomial functions for scenario 2. For a

Scenario	\mathcal{P}	Ω	$PLAV$	$PLSV$	$SLAV$	$SLSQ$	NN_A	NN_B
1	[1.5, 1.5, 1.5]	[1.5, 3.0, 4.5]	28.31	33.92	12.54	13.12	11.25	10.15
2	[2.0, 2.0, 2.0]	[2.0, 4.0, 6.0]	18.94	20.38	13.48	11.70	15.76	10.10
3	[2.5, 2.5, 2.5]	[2.5, 5.0, 7.5]	20.58	25.00	20.92	17.95	15.70	10.88
4	[1.5, 1.5, 1.5]	[2.5, 4.0, 6.0]	32.04	28.50	10.01	14.47	16.2	14.25
5	[2.0, 2.0, 2.0]	[2.5, 4.0, 6.0]	25.67	22.01	12.54	14.47	17.56	14.25
6	[2.5, 2.0, 1.5]	[2.5, 4.0, 6.0]	21.46	20.21	7.01	10.51	6.75	7.25
7	[2.5, 2.0, 1.5]	[2.5, 3.5, 4.0, 4.5, 6.0]	45.63	49.21	34.96	45.38	27.69	25.01

Table 1: Confusion (%) in training stage for the heating scenarios

Scenario	\mathcal{P}	Ω	$PLAV$	$PLSV$	$SLAV$	$SLSV$	NN_A	NN_B
8	[0.5, 0.5, 0.5]	[0.5, 1.0, 1.5]	30.15	33.23	12.26	12.73	16.11	17.16
9	[1.0, 1.0, 1.0]	[1.0, 2.0, 3.0]	18.28	19.33	10.63	9.33	19.42	8.35
10	[1.5, 1.5, 1.5]	[1.5, 3.0, 4.5]	23.40	25.75	21.61	18.00	13.54	13.13
11	[0.5, 0.5, 0.5]	[1.5, 2.0, 3.0]	31.32	36.23	12.69	19.42	9.57	9.14
12	[1.0, 1.0, 1.0]	[1.5, 2.0, 3.0]	22.08	22.44	13.96	13.74	5.36	12.40
13	[1.5, 1.0, 0.5]	[1.5, 2.0, 3.0]	22.18	24.24	8.03	11.17	22.71	13.19
14	[1.5, 1.0, 0.5]	[1.5, 2.0, 2.5, 3.0]	46.53	46.84	39.19	44.61	26.84	23.38

Table 2: Confusion (%) in training stage for the cooling scenarios

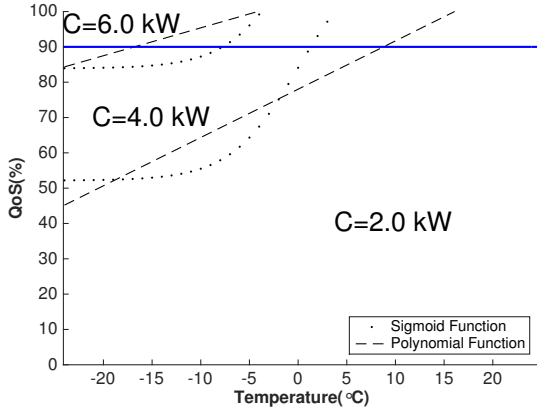


Figure 7: Comparison of sigmoid and polynomial areas for scenario 2.

QoS of 90%, we see that the polynomial function gives a transition between areas either before or after the sigmoid function. If it is before, $T \in (-18, -8)^\circ\text{C}$, we will obtain a worse QoS and lower temperatures in the rooms. If it is after, $T \in (2, 8)^\circ\text{C}$, we will have extra capacity that is not required. This lower utilization of the capacity becomes more important if the user is paying in advance for a re-410 source that will not be used.

On the other hand, scenarios 7 and 14 are significantly different: the NNs have considerably better performance than any other approach. Looking deeper into the characteristics of these scenarios we see a special condition: sev-415 eral values in Ω can generate the same QoS at the same temperature. We may have the same performance in scenario 7 for $\omega = 4$ and $\omega = 4.5$ if the three heaters send

requests at the same time. In the first case, the AC will accept P_1 and P_3 and leave P_2 for the next time step. In the second case the order of acceptance changes but the QoS is the same. Figure 8 shows the training set for this scenario; we can see how $C = 4$ is distributed over its adjacent classes.

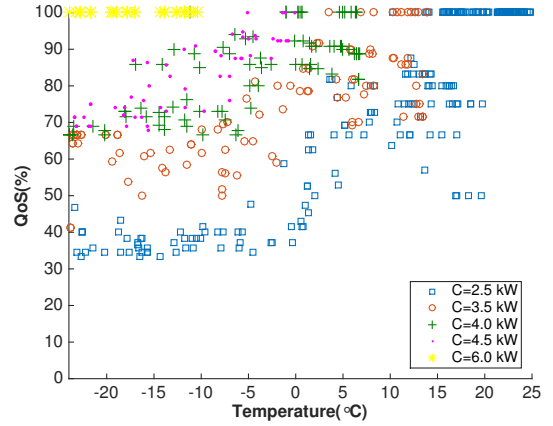


Figure 8: Training data for scenario 7 (heating).

Although the NNs have a better training performance, they might minimize the confusion value by eliminating one of the classes. Let W_ω be the set of points that belong to class ω , and let W_ω^1 and W_ω^0 be the subsets of points correctly and incorrectly classified respectively. Let Γ be the total number of misclassified points. The approach presented in this article separates any two contiguous sets following the fitted function, and therefore $W_1^1 + W_1^0 = |W_1|$, $W_2^1 + W_2^0 = |W_2|$, and $W_1^0 + W_2^0 = \Gamma$.

If we assume that the NN eliminates class 2 we have $\bar{W}_1^1 = |W_1|$, $\bar{W}_2^0 = |W_2|$, and $W_2^1 + W_2^0 = |W_2| = \bar{\Gamma}$. We can conclude that eliminating one class improves the confusion (i.e., $\bar{\Gamma} < \Gamma$) if $W_2^1 < W_1^0$.

At this point we can see the advantage of exploiting the features of the problem. In the approach presented in this paper the fitted function acts as a constraint that represents the structure of the data sets. On the other hand, the flexibility of the NNs allows a lower misclassification, but we see in Subsection 3.2 that this has an unexpected impact on the QoS .

3.2. Results for Three-Load Instance

The experiments use data for a period of two years (2014 and 2015) for the Montreal area (17520 data points). The user sets a QoS of 90%. Figures 9–14 show the results for scenarios 2 and 7 (heating) and scenario 14 (cooling). These box plots contain the minimum value, maximum value, and interquartile range for the hourly QoS and the hourly average temperature in the three rooms for each of the methods compared.

For scenario 2 (Figures 9 and 10) we see that the sigmoid and NN cases perform slightly better than the polynomial function. Although the QoS and the temperature do not vary significantly, the use of the resource differs: the polynomial function reports around 60% of utilization of capacity while the other four methods achieve a utilization between 70% and 75%. This effect was previously observed in Figure 7. Scenarios 1, 3 to 6, and 8 to 13 have similar results.

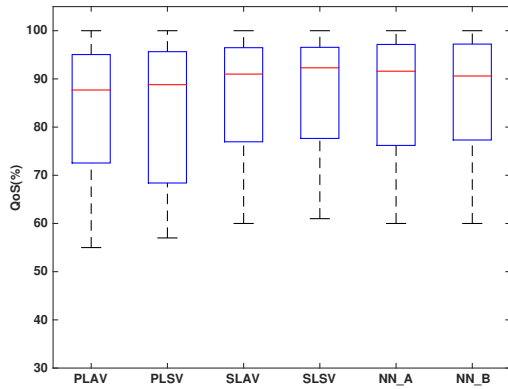


Figure 9: QoS test results for scenario 2 (heating).

In the case of scenarios 7 and 14 we observe a special situation: although the training results for the NNs are better we have a worse QoS (Figures 11 and 13) and temperature management (Figures 12 and 14). We previously saw in Figure 8 that the areas for classes 3.5, 4, and 4.5 are not clearly defined. We also saw that different capacities can result in a similar QoS at the same temperature

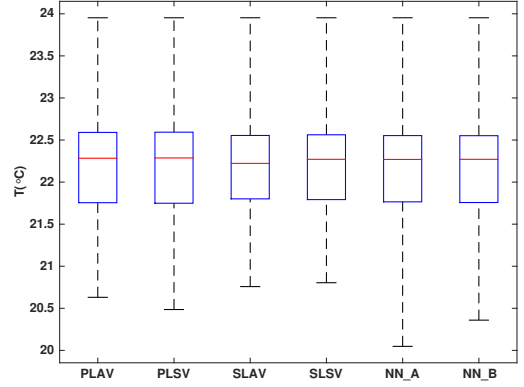


Figure 10: Average room temperature test results for scenario 2 (heating).

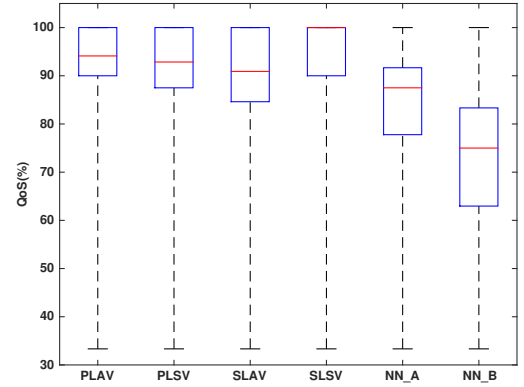


Figure 11: QoS test results for scenario 7 (heating).

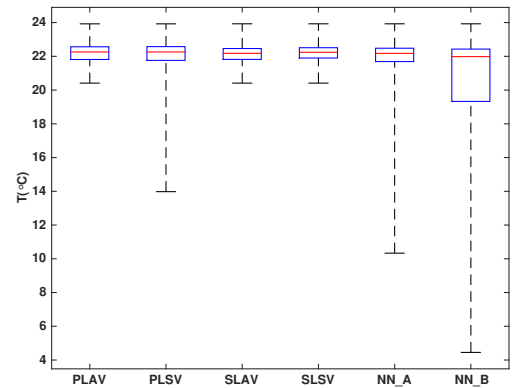


Figure 12: Average room temperature test results for scenario 7 (heating).

due to the load shifting. Nevertheless, eliminating one of the classes can have negative effects on the final output;

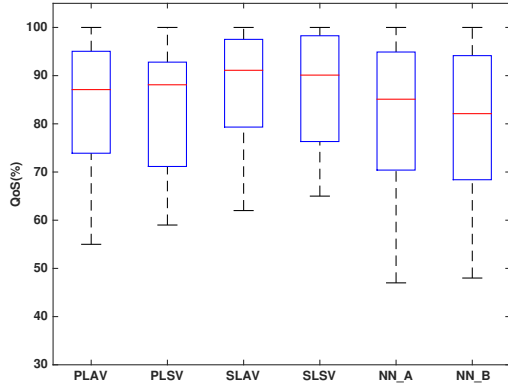


Figure 13: QoS test results for scenario 14 (cooling).

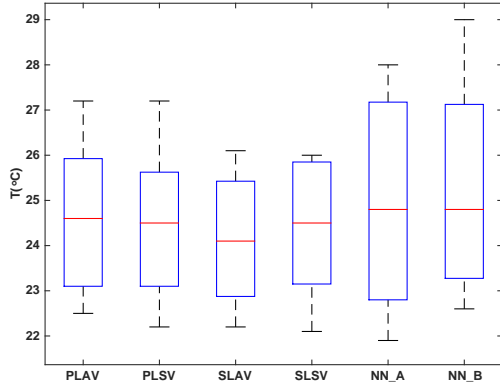


Figure 14: Average room temperature test results for scenario 14 (cooling).

in this case the NNs tend to eliminate class 4.5 in order to minimize the confusion value. Although $C = 4.5$ and $C = 4.0$ can accept two out of the three loads if all of them arrive at the same time, the situation changes when the loads arrive at different times. For example, $C = 4.5$ will satisfy any of the combinations of two loads arriving simultaneously: $[2.0, 2.5]$, $[1.5, 2.5]$, and $[1.5, 2.0]$, whereas $C = 4.0$ will not accept $[2.0, 2.5]$. It is therefore preferable not to eliminate a class because of the dynamics in the system.

3.3. Results for Fifty-Load Instance

To demonstrate the scalability of the proposed methodology, we present results for an instance with 50 space heaters. This instance represents an apartment building with three different types of heaters $\mathcal{P} = [1.5, 2.0, 2.5]$ with respectively 20, 15, and 15 loads of each type. We consider the scenario in which the building operator chooses $\Omega = [25.0, 45.0, 70.0, 90.5]$. Figures 15–17 give a summary of the results.

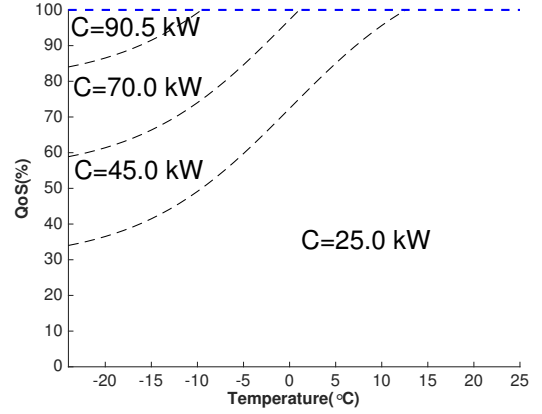


Figure 15: Classification areas.

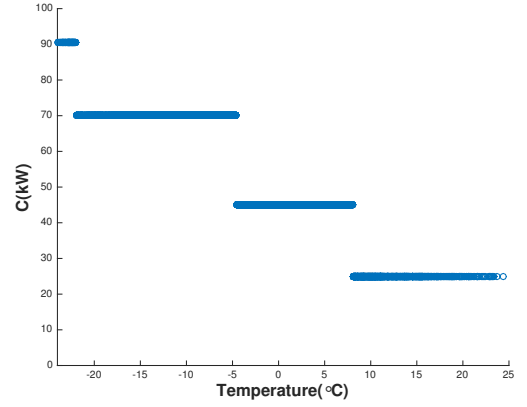


Figure 16: Capacity as function of external temperature.

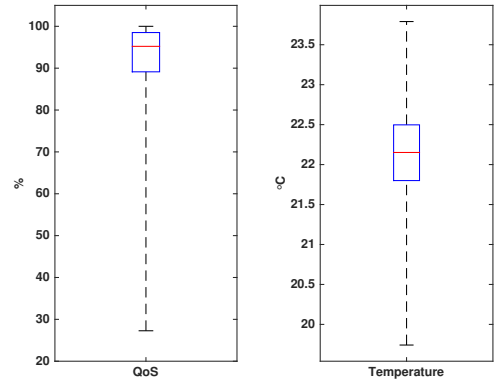


Figure 17: Average QoS and average room temperature.

Figure 15 shows that the classification areas have the expected sigmoid shape. Figure 16 shows that as the external temperature increases, the capacity required decreases. Finally, Figure 17 shows that the average QoS and the average room temperature remain in the comfort zone.

An important feature of this novel approach is that the QoS aggregates all the requests from the loads. Therefore,

regardless of the size of the population, it maintains the asymptotic and monotonic increasing behavior explained previously.

4. Conclusions

Understanding the requirements of residential consumption is key to facilitating increased participation in DR programs. The methodology proposed in this paper computes a power capacity profile that meets the user's expectations and at the same time provides information to residential power management systems. The use of the AC and the implementation of the *QoS* index allow us to aggregate a set of loads, simplifying the decision-making process.

The approach we have presented takes advantage of the inner structure of the defined problem, ensuring a good representation of the historical data and a reliable tool for future estimation. The shaving effect can be achieved, controlling the peak consumption, respecting the *QoS*, and ensuring a better utilization of the power capacity available.

The proposed method computes capacity profiles for a specific comfort zone with a defined set of loads. For different configurations of the building and/or different boundary conditions, the user can easily compute the new classification areas for different scenarios and intervals of comfort. The quality of the historical data and coherence in the thermal system when defining the set of loads are key to the applicability of this method.

Future work will explore the applicability of the proposed methodology to more complex systems with different types of buildings and loads and also take into account the user behavior.

Finally, the approach presented is computationally efficient, it utilizes data that is normally available in the smart building context, and it performs well for heating and cooling, offering better performance than NNs in a real-world-based scenario.

Acknowledgments

We thank the editor and the two anonymous referees for their detailed and helpful comments on earlier versions of this paper.

This research was supported by the *Canada Research Chair on Discrete Nonlinear Optimization in Engineering*.

References

- [1] Electric Power Annual 2014, Tech. rep., U.S. Energy Information Administration (2016).
- [2] Households and the Environment: Energy Use, Tech. rep., Statistics Canada (2013).
- [3] 2014 Yearbook of Electricity Distributors, Tech. rep., Ontario Energy Board (2015).
- [4] Survey of Household Energy Use, Tech. rep., Natural Resources Canada (2011).
- [5] G. T. Costanzo, G. Zhu, M. F. Anjos, G. Savard, A system architecture for autonomous demand side load management in smart buildings, *IEEE Transactions on Smart Grid* 3 (4) (2012) 2157–2165.
- [6] K. Margellos, S. Oren, Capacity controlled demand side management: A stochastic pricing analysis, *IEEE Transactions on Power Systems* 31 (1) (2016) 706–717.
- [7] S. Rahim, N. Javaid, A. Ahmad, S. A. Khan, Z. A. Khan, N. Alrajeh, U. Qasim, Exploiting heuristic algorithms to efficiently utilize energy management controllers with renewable energy sources, *Energy and Buildings* 129 (2016) 452–470.
- [8] D. Caprino, M. L. D. Vedova, T. Facchinetti, Peak shaving through real-time scheduling of household appliances, *Energy and Buildings* 75 (2014) 133–148.
- [9] X. Li, H. H. Chen, X. Tao, Pricing and capacity allocation in renewable energy, *Applied Energy* 179 (2016) 1097–1105.
- [10] G. L. Doorman, Capacity subscription: Solving the peak demand challenge in electricity markets, *IEEE Transactions on Power Systems* 20 (1) (2005) 239–245.
- [11] T. Logenthiran, D. Srinivasan, T. Z. Shun, Demand side management in smart grid using heuristic optimization, *IEEE Transactions on Smart Grid* 3 (3) (2012) 1244–1252.
- [12] A. Ogunjuyigbe, T. Ayodele, O. Akinola, User satisfaction-induced demand side load management in residential buildings with user budget constraint, *Applied Energy* 187 (2017) 352–366.
- [13] L. Suganthi, A. A. Samuel, Energy models for demand forecasting: A review, *Renewable and Sustainable Energy Reviews* 16 (2) (2012) 1223–1240.
- [14] L. G. Swan, V. I. Ugursal, Modeling of end-use energy consumption in the residential sector: A review of modeling techniques, *Renewable and Sustainable Energy Reviews* 13 (8) (2009) 1819–1835.
- [15] K. Ahmed, M. Ampatzis, P. Nguyen, W. Kling, Application of time-series and artificial neural network models in short term load forecasting for scheduling of storage devices, in: *Power Engineering Conference (UPEC), 2014 49th International Universities*, 2014, pp. 1–6.
- [16] R. K. Jain, K. M. Smith, P. J. Culligan, J. E. Taylor, Forecasting energy consumption of multi-family residential buildings using support vector regression: Investigating the impact of temporal and spatial monitoring granularity on performance accuracy, *Applied Energy* 123 (2014) 168–178.
- [17] A. Al-Wakeel, J. Wu, N. Jenkins, k-means based load estimation of domestic smart meter measurements, *Applied Energy* (2016) –doi:<http://dx.doi.org/10.1016/j.apenergy.2016.06.046>.
- [18] R. Subbiah, K. Lum, A. Marathe, M. Marathe, Activity based energy demand modeling for residential buildings, in: *Innovative Smart Grid Technologies (ISGT), 2013 IEEE PES*, 2013, pp. 1–6.
- [19] J. Massana, C. Pous, L. Burgas, J. Melendez, J. Colomer, Short-term load forecasting in a non-residential building contrasting models and attributes, *Energy and Buildings* 92 (2015) 322–330.
- [20] S. Mohajeryami, M. Doostan, A. Asadinejad, P. Schwarz, Error analysis of customer baseline (CBL) calculation methods for residential customers, *IEEE Transactions on Industry Applications* 53 (1) (2017) 5–14.
- [21] H. Zareipour, A. Janjani, H. Leung, A. Motamedi, A. Schellenberg, Classification of future electricity market prices, *IEEE Transactions on Power Systems* 26 (1) (2011) 165–173.
- [22] H. Zareipour, D. Huang, W. Rosehart, Wind power ramp events classification and forecasting: A data mining approach, in: *2011 IEEE Power and Energy Society General Meeting*, 211, pp. 1–3.
- [23] D. Cluwin, Demand response and storage for demand side management in smart buildings, Internship report, University of Twente and Polytechnique Montreal (April 2014).
- [24] M. Kuzlu, M. Pipattanasomporn, S. Rahman, Hardware demonstration of a home energy management system for demand response applications, *IEEE Transactions on Smart Grid* 3 (4) (2012) 1704–1711.
- [25] Historical climate data, <http://climate.weather.gc.ca>, [Gov-

erment of Canada; accessed July 2016].

- [26] B. Olesen, K. Parsons, Introduction to thermal comfort standards and to the proposed new version of EN ISO 7730, *Energy and Buildings* 34 (6) (2002) 537–548, special Issue on Thermal Comfort Standards.
- [27] N. V. Chawla, Data mining for imbalanced datasets: An overview, in: O. Maimon, L. Rokach (Eds.), *The Data Mining and Knowledge Discovery Handbook*, Springer US, Boston, MA, 2005, pp. 875–886.
- [28] T. E. Dielman, A comparison of forecasts from least absolute value and least squares regression, *Journal of Forecasting* 5 (3) (1986) 189–195.